N90-17905

A MULTICOLOR IMAGING PYROMETER

Michael B. Frish and Jonathan H. Frank

Physical Sciences Inc.
Research Park, PO Box 3100, Andover MA 01810

1. INTRODUCTION

Pyrometry is a well-established technique for determining the temperature of a material by measuring the radiation that it emits. In general, the accuracy of pyrometry suffers from the problem that there is always one parameter which must be known to determine the temperature but cannot be measured. This parameter is usually the emissivity of the material at a specific wavelength or the ratio of emissivities at two or more different wavelengths. In most materials the emissivity changes as the material is heated, and easily made measurements of the emissivity at room temperature provide little information that is useful at elevated temperatures. Therefore, an educated guess of the material's high temperature emissivity must be made. The accuracy of this guess determines the resultant accuracy of the temperature measurement.

Recently, a new technique has been developed for using pyrometry to measure elevated temperatures with a minimum of emissivity related uncertainty.[1-4] The approach utilizes an optical system that collects radiation emitted at a wavelength that is short compared to the peak of the blackbody spectrum for the temperature range of interest. In this regime the radiant power increases faster than exponentially with temperature. Because of this extreme sensitivity to temperature, the emissivity of the source plays a relatively small role in determining the emitted power. Such a pyrometer therefore provides a more accurate measurement of the temperature than one using a longer wavelength. However, because the dynamic range of the photodetector usually places rather narrow limits on the range of temperatures that can be measured at a single short wavelength, to cover a broad range of temperatures it is valuable to provide several different detectors, each sensitive to a different wavelength and to a specific temperature range. Such a device is herein called a multicolor pyrometer.

This multicolor approach has now been incorporated into an imaging pyrometer designed to measure the temperatures distributions along the surfaces of small (~2 mm diameter) moving objects subjected to radiant heating in a furnace. As reported herein, this device is capable of measuring temperatures between 1000 and 2500K with better than 0.2 percent precision and an emissivity-related temperature uncertainty which is less than 10 percent of the emissivity uncertainty. In its present configuration, the system updates the temperature map at a rate of about 10 Hz and has a spatial resolution of about 0.1 mm.

The theory underlying the design of the multicolor pyrometer is discussed in Section 2 below. This is followed by a detailed description of the imaging system in Section 3, and its operation in Section 4. Section 4 also reports the successful results of an experiment validating the pyrometer's accuracy and precision. The paper concludes with a summary in Section 5.

2. THEORY

2.1 The Accuracy of Multicolor Pyrometry

The radiant energy emitted by any object is determined by the Planck equation:[5]

$$R(\lambda)d\lambda = \frac{C_1}{\pi\lambda^5} \frac{\varepsilon(\lambda,T)\, d\lambda}{\exp(C_2/\lambda T) - 1} \qquad (1)$$

where $R(\lambda)d\lambda$ is the radiant flux per steradian per unit area of emitter surface in the wavelength interval $[\lambda, \lambda + d\lambda]$, $C_1/\pi = 1.191 \times 10^{-12}$ W-cm^2/sr, $C_2 = 1.44$ cm-K, T is the temperature, and $\varepsilon(\lambda,T)$ is the spectral emissivity of the material at wavelength λ. In a typical pyrometer, a portion of the heated target's surface is imaged by a group of lenses and mirrors onto a photodetector which converts the incident radiation into a measurable electrical quantity. The optical path generally contains several windows, mirrors, beam splitters or filters, each of which has a wavelength dependent transmittance or reflectance, $t_i(\lambda)$. They, together with the solid angle Ω subtended by the optical collection system, and the surface area, A_s, of the radiant target, determine the radiant power which reaches the detector,

$$P = \frac{A_s \Omega C_1}{\pi} \int_0^\infty \frac{\prod_{i=1}^{n} t_i(\lambda)\varepsilon(\lambda,T)d\lambda}{\lambda^5[\exp(C_2/\lambda T)-1]} \qquad (2)$$

where n is the number of components in the optical train. By using a narrow bandpass optical filter to select a particular wavelength (i.e., color) at which to measure the radiance, the emissivity of the target and the transmittance or reflectance of other optical components are essentially constant over the bandpass. These

variables can therefore be removed from the integral in Eq.(2) and, if the transmission curve of the filter is known, the integral may be evaluated, as

$$P = \varepsilon_\lambda D_\lambda \int_{\lambda_1}^{\lambda_2} \frac{t_f(\lambda)d\lambda}{\lambda^5[\exp(C_2/\lambda T) - 1]} \tag{3}$$

where ε_λ is the emissivity at the central wavelength of the filter, D_λ is a constant (independent of temperature) determined by the optical system which may be evaluated by calibration, t_f is the (known) transmission function of the filter, and λ_1, λ_2 are the bandpass limits of the filter. When the photodetector is operated such that it generates a voltage signal which is proportional to the energy incident on its surface during a period of time τ, Eq. (3) may be written as

$$V(T) = \varepsilon_\lambda B_\lambda F_\lambda(T) \tag{4}$$

where $F_\lambda(T)$ is a known thermal response function proportional to the integral in Eq. (3), and

$$B_\lambda = GD_\lambda \eta_\lambda \tau \tag{5}$$

where G (volts/coulomb) is the responsivity of the photodetector and its associated amplification circuitry, and η_λ (coulombs/joule) is proportional to the quantum efficiency of the detector.

Unfortunately, in addition to its dependence on temperature, the radiant emission from a heated object at a given wavelength depends on its emissivity, an intrinsic property of the material. Furthermore, as indicated in Eq. (1), the emissivity may be a function of both wavelength and temperature. It may also change with time as a material suffers changes in its transparency, reflectivity, or surface structure due to phase changes, chemical reaction, ablation, etc. Thus, the wavelength and temperature dependences of the emissivity are often unknown, and precise pyrometric measurement of the true temperature in such situations is generally accepted as being essentially impossible.

By always operating the pyrometer at a wavelength such that $\lambda T << 1$ cm-K, the multicolor technique described herein provides the best possible estimate of the true temperature under the difficult circumstances of unknown and unmeasurable emissivities which vary wildly and unpredictably with wavelength, temperature, and time. Eq. (1) shows that, at these short wavelengths, the radiant power emitted by a heated surface increases faster than exponentially with temperature, but is only linearly dependent on emissivity. Thus, a large uncertainty in emissivity causes only a small error in temperature. Mathematically, this is seen by solving Eq.(4) for temperature. The function $F_\lambda(T)$ may be easily evaluated by approximating the transmission function of the narrow bandpass filter by a rectangle of height t_λ and width $\Delta\lambda = \lambda_2 - \lambda_1$. Defining

$$P_\lambda(T) = \{\exp(C_2/\lambda T) - 1\}^{-1} \tag{6}$$

and

$$B_\lambda = \frac{A_s \Omega t_\lambda \eta_\lambda \tau G C_1 \Delta\lambda}{\pi\lambda^5} \prod_{i=1}^{n} t_i \tag{7}$$

and solving Eqs. (4) through (7) for temperature yields

$$T = \frac{C_2}{\lambda \ln\{(B_\lambda \varepsilon_\lambda / V) + 1\}} \quad . \tag{8}$$

Differentiating with respect to ε_λ gives the temperature accuracy as

$$\frac{\Delta T}{T} = [\, 1 - \exp(-C_2/\lambda T)] \; \frac{\lambda T}{C_2} \frac{\Delta\varepsilon_\lambda}{\varepsilon_\lambda} \tag{9}$$

which is plotted in Figure 1 for several wavelengths using $\Delta\varepsilon_\lambda/\varepsilon_\lambda = \pm 0.25$. Although the temperature uncertainty increases with temperature for all wavelengths, it is clear that, by selecting a sufficiently short wavelength for operation of the pyrometer, uncertainties of less than two percent can be achieved.

2.2 Practical Considerations

On the basis of Eqs. (8) and (9), it would appear that a single color pyrometer could be used to measure any temperature below a predetermined value to any degree of accuracy simply by selecting a sufficiently short wavelength. Although this is true in principle, either detector sensitivity or shot noise places a lower limit on the temperature sensitivity for any particular wavelength and optical collector combination. In addition, there is a maximum temperature to which a particular system will be sensitive, fixed by the onset of detector saturation. Photodetectors used in typical imaging systems have a dynamic range of only about two orders of magnitude. However, at 370 nm, where the temperature accuracy is ±40K when the true temperature is 2500K and the emissivity error is ±25 percent, the radiant power spans a dynamic range exceeding ten orders of magnitude as the temperature increases from 1000 to 2500K. A single imaging pyrometer operating at this

wavelength is clearly unsuitable for measurements over this entire temperature range. Longer wavelengths cannot be used at the higher temperatures without sacrificing accuracy. However, if use of this short wavelength is limited to temperatures between about 2250 and 2500K, the dynamic range required of the detector is less than 10. An additional detector operating at 420 nm and otherwise having the same sensitivity and dynamic range is able to measure temperatures between 1970 and 2250K while retaining the accuracy of the shorter wavelength detector. Thus, by using several individual different-color pyrometers, the entire temperature range of interest can in principle be measured with high accuracy, assuming only marginal knowledge of the emissivity. Thus, a multicolor pyrometer is considered here to be a group of single color pyrometers of which only one is used at a time. As described next, we have utilized this approach to assemble a multicolor imaging pyrometer.

3. MULTICOLOR IMAGING PYROMETER

3.1 Description

The imaging pyrometer was designed to measure surface temperature distributions of objects having diameters of at least 2 mm moving within a spherical volume of about 1 cm diameter. As illustrated schematically in Figure 2, radiation emitted by the heated sample is collected by a 360 mm focal length objective lens which, since the sample is located within the focal plane of the objective, projects a nearly collimated beam into a color separator. Six different-color images are then projected onto a single charged-coupled-device (CCD) photodetector array.

The color separation is accomplished using a series of dichroic beamsplitters, of which three are shown in Figure 2. The first beamsplitter ideally reflects all radiation at wavelengths greater than λ_1 while transmitting all shorter wavelengths. The second beamsplitter similarly reflects all radiation at wavelengths longer than λ_2 (of which there is ideally none longer than λ_1) and transmits the rest, which is reflected by the third mirror. The three reflected beams are transmitted through interference filters, which select the desired narrow bands of wavelengths from the relatively broad bands reflected by the beamsplitters, and thence through 100 mm focal length lenses which image the sample onto the CCD array located at the focal plane of the lenses. To provide all six images, a fourth dichroic beamsplitter is inserted ahead of the three shown. It reflects a band of wavelengths upwards to a second row of beamsplitters. The reflections from this second layer are projected similarly onto the CCD, as illustrated by the side view of Figure 3. The optical collection efficiency of the system is limited by the 25 mm diameter imaging lenses to about F/14. To reduce optical aberrations, it is preferable to place a stop at the objective lens limiting the speed to F/18. When operating at this speed there is no vignetting of objects moving within the field of view. The overall system magnification of 0.28 is determined by the ratio of the focal lengths of the objective lens to the imaging lenses.

The six optical paths are aligned so that the centers of the images are positioned on the CCD as illustrated in Figure 4. Each center is 1.5 mm from its neighbors, meaning that objects 1.5/.28 = 5.3 mm in diameter can be observed without the images overlapping each other. Since the image centers are also at least 1.5 mm from the edge of the detector, each image is a projection of the full 1 cm field of view.

The CCD detector divides the images into an array of 610 x 244 pixels, each of which can be considered to be an individual photodetector. The associated electronics, incorporated into a Sierra Scientific Model 4032 camera, convert the irradiance incident on each pixel during a fixed exposure period into a voltage value, and transmits the voltage values sequentially in an RS-170 video format. That is, each horizontal line of pixels is transmitted during a 63.5 μs period, and all 244 lines are transmitted every 1/60 s, thereby comprising a video field. A unique feature of this camera is its capability to alter the exposure time to any value between 1 and 1000 ms while maintaining the RS-170 format. Each video field is acquired by a Data Translation Model 2851 frame grabber, which digitizes the transmitted data with 8-bit accuracy, stores it in an on-board buffer or transfers it to the Compaq 286 personal computer memory, and displays it on a video monitor. The computer and frame-grabber, functioning together, are programmed to select which one of the six available images contained within the frame provides data that is suitable for conversion to temperature values, performs the conversion, and displays the results as a false color temperature map. The map can be updated 10 times per second, and the data can be stored on videotape for post-test analysis.

3.2 Wavelength Selection

The six wavelengths used in the pyrometer have been selected to provide high measurement precision while spanning a temperature range from less than 1000K to greater than 2500K. The longest wavelength provides measurement of the lowest temperature possible with this system, determined as follows: The minimum temperature detectable at any given wavelength is that which, during the exposure time, generates a signal equal to the detector's rms noise. In general, as the wavelength increases the associated minimum detectable temperature decreases, and conversely as the temperature decreases the optimum wavelength for measuring it increases. However, at long wavelengths the quantum efficiency of the detector decreases with increasing wavelength, resulting in the existence of a temperature below which no signal can be detected regardless of the wavelength. This is the minimum measurable temperature and, for our system, has been calculated to be 888K at a wavelength of 930 nm assuming an exposure time of 50 ms. The maximum temperature observable at this wavelength, i.e. that which saturates the detector, is 1302K.

All of the other colors were chosen to provide a precision better than 0.2 percent during a 16.67 ms exposure at a minimum temperature equal to the maximum temperature observable with the next longest wavelength. The precision of the temperature measurement is, in essence, determined by the 8-bit precision of the video frame grabber, in which the minimum resolvable change in signal is $1/(2^8-1) = 1/255$ of the signal at saturation. Each 1-bit signal change is called a gray level. Because the signal generated at a specific wavelength increases much more rapidly than linear with increasing temperature, the precision of the measurement also increases with temperature. That is, at higher temperatures a smaller change in temperature is required to produce an incremental step in the gray level than at lower temperatures. Thus, the minimum temperature at which a specified precision can be achieved may correspond to a gray level greater than unity,

and therefore is higher than the minimum detectable temperature. Each color therefore has both a wavelength and a minimum gray level specified for optimum precision. The selected colors, the range of temperatures spanned by each color while providing a measurement precision of 0.2 percent, and the ranges measurable regardless of precision are shown in Table 1. The ratio of temperature uncertainty to the emissivity uncertainty at the peak temperature of each color is also tabulated.

TABLE 1

Wavelength (nm)	High Temp. (K)	Low Temp. @ 0.2 % Precision	Minimum Detectable Temperature	$\frac{\Delta T/T}{\Delta \varepsilon/\varepsilon}$
930	1302	1119	888	0.08
750	1506	1298	1050	0.08
590	1728	1505	1244	0.07
480	1971	1726	1445	0.07
420	2249	1970	1650	0.07
370	2562	2243	1878	0.07

The temperature ranges shown in Table 1 assume a sample emissivity of 0.5. Figure 5 graphically displays the range of temperatures measurable with 0.2 percent precision at each of these wavelengths as a function of emissivity. The minimum temperature measurable at the longest wavelength regardless of precision is also shown. In the shaded regions the upper range of one filter overlaps with the lower range of the filter of next shorter wavelength. The overlap has been designed to be only a few degrees at each transition, but can be enhanced by decreasing the lower temperature limits of each color, either by increasing the integration time, or by decreasing the precision. Thus, through the use of the computer controlled variable integration time camera and these filters, wide flexibility in the the operation of the system is possible.

4. PYROMETER OPERATION

4.1 Data Acquisition and Processing Algorithms

Four steps are required for each update of the temperature map acquired and displayed with the pyrometer: 1) acquiring a field of data; 2) subtracting the dark signal from that field; 3) selecting the appropriate one of the six available images for analysis; and 4) converting the radiance data in the image to temperature values. The last step assumes, of course, that the system has been precalibrated so that the correspondence between measured radiance and temperature is known.

Acquisition of the video field is performed by straightforward programming of the frame grabber. The video signal is digitized and stored in one of the on-board frame buffers. To convert this information into accurate temperature data, the dark signal is subtracted from each field of data. Each pixel in the field has a unique dark signal that is a function of the integration time and is measured simply by blocking the pyrometer's entrance aperture, adjusting the integration time to the desired value, and averaging a sequence of 100 frames. Average values of the gray level at each pixel are then stored in an auxiliary frame buffer and called up as required for background subtraction.

As described above, the pyrometer projects six non-overlapping images onto the CCD array simultaneously, but only one image provides data suitable for reduction to temperature. All of the other images are either bright enough to saturate the frame grabber, or dim enough to be undetectable. Selection of the correct image is accomplished by scanning predetermined portions of the video field to locate pixels which have non-zero but unsaturated gray levels. To this end, an algorithm has been developed that locates the centroid of the longest wavelength image, and checks to determine whether it is saturated. If it is saturated, then the center of the image corresponding to the next longest wavelength, located 1.5 mm away from the first image, is checked for saturation. This procedure is repeated until an unsaturated image is found, which, by design, must be the one that provides valid data.

The pyrometer is calibrated by placing a source (such as a blackbody) of known temperature and emissivity in the object plane, measuring the most probable gray level of the image at the appropriate wavelength, determining the calibration constant defined by Eq. (4), and finally using the Planck equation to generate a lookup table relating each of the 256 avaliable gray levels within the image to a corresponding temperature. The lookup table is stored for use during data acquisition.

The temperature measurement procedure combines all of the steps described above. A video field containing the six images of the hot moving object is acquired and stored in a frame buffer. The appropriate image is then located and the background subtracted. The result is passed through an output lookup table which displays on the video monitor a false color image corresponding to the temperature distribution in the object. This lookup table may be the one created during the calibration procedure, or it may be a modified version that accounts for any user knowledge of the object's emissivity. In addition to displaying a temperature map, the algorithm finds the maximum temperature within the object and displays this value in numerical form. This value may also be used in a feedback loop to actively control the temperature.

4.2 Demonstration

A breadboard version of the multicolor imaging pyrometer has been used to measure the temperature of a low emissivity surface, namely molten aluminum contained in a clear quartz crucible, subjected to radiant

heating within a kiln and observed through a small port in the kiln's wall, as illustrated in Figure 6. Under these conditions, the radiation seen by the pyrometer is a combination of the radiation emitted by the aluminum and that emitted by the kiln walls at temperature T_w and reflected from the aluminum surface at T_s:

$$R(\lambda)d\lambda = \frac{c_1}{\pi\lambda^5}\left[\frac{\varepsilon_s(\lambda,T_s)}{\exp(c_2/\lambda T_s) - 1} + \frac{1 - \varepsilon_s(\lambda,T_s)}{\exp(c_2/\lambda T_w) - 1}\right] . \quad (10)$$

The second term, which accounts for the reflected radiation, depends on the background temperature and the sample emissivity. This is simply a result of energy conservation, which requires the sum of the monochromatic reflectivity, transmitivity and absorptivity of a material to equal unity, and Kirchoff's law which, in a simple form, states that the absorptivity of a material, at a given wavelength, is equal to its emissivity. Thus, $1-\varepsilon_s(\lambda,T_s)$ is equal to the reflectivity of the aluminum and is the proper factor to use for incorporating the background radiation effects.

In these experiments, because the heating rate is slow, the aluminum and the walls of the kiln are at roughly the same temperatures, i.e. $T_w \approx T_s$. As a result, the radiation observed is approximately that of a blackbody at T_s. The pyrometer was therefore programmed to assume an emissivity of unity. The temperature of the aluminum, as it heated from room temperature to about 1000C, was monitored by the pyrometer. A thermocouple was suspended within the crucible to measure the aluminum's temperature directly. Figure 7 is a comparison of the average temperature observed by the pyrometer with that of the thermocouple. The agreement is essentially perfect within the precision of the pyrometer's measurement capabilities.

5. SUMMARY

A multicolor imaging pyrometer has been designed for accurately and precisely measuring the temperature distribution histories of small moving samples. The device projects six different color images of the sample onto a single CCD array that provides an RS-170 video signal to a computerized frame grabber. The computer automatically selects which one of the six images provides useful data, and converts that information to a temperature map. By measuring the temperature of molten aluminum heated in a kiln, a breadboard version of the device has been shown to provide high accuracy in difficult measurement situations. It is expected that this pyrometer will ultimately find application in measuring the temperatures of materials undergoing radiant heating in a microgravity acoustic levitation furnace.

References

1. M.B. Frish, "Measurement of High Temperature Thermophysical Properties with Electron Beam Heating," AIAA Paper No. 84-1784 (1984).

2. M.B. Frish, M.N. Spencer, N.E. Wolk, J.S. Werner and H.A. Miranda, "Multi-Color Pyrometer for Materials Processing in Space", Proc. of the Noncontact Temperature Measurement Workshop, NASA Conf. Pub. 2503 (May 1987).

3. P.C. Nordine, "The Accuracy of Multicolor Optical Pyrometry", High Temperature Science, 21, (1986).

4. D.P. DeWitt and R.E. Rondeau, "Evaluation of a Method for Measuring Front-Face Surface Temperatures and Spectral Emissivities During Irradiation", AIAA Paper No. 87-1565 (1987).

5. Siegel, R. and Howell, J.R., Thermal Radiation Heat Transfer, McGraw-Hill (1981).

Acknowledgment

Support for this work from the NASA Jet Propulsion Laboratory, under SBIR contract NAS7-1002, is gratefully acknowledged.

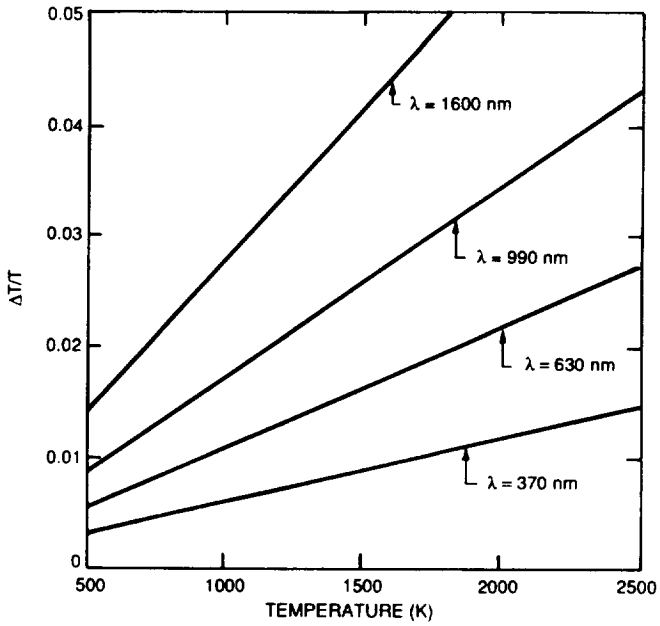

Figure 1. Temperature uncertainties resulting from an emissivity uncertainty of $\Delta\varepsilon/\varepsilon = \pm 0.25$ at several wavelengths.

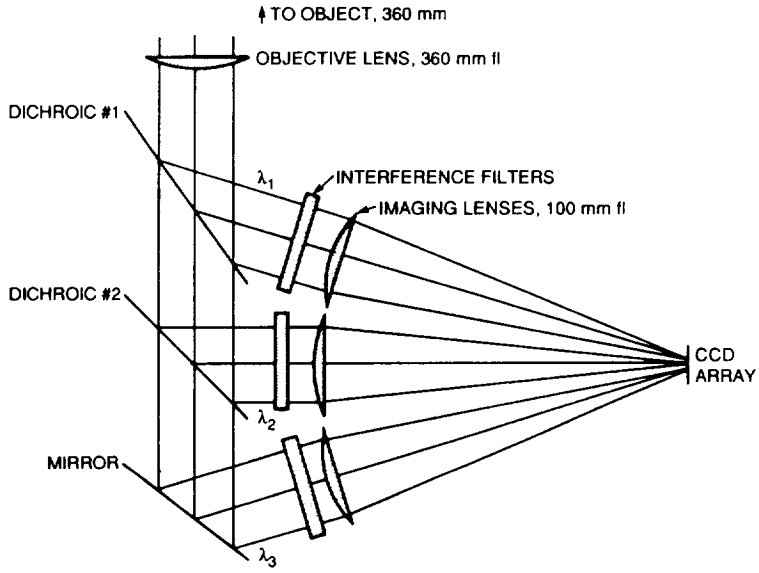

Figure 2. Schematic illustration of multicolor pyrometer optical configuration.

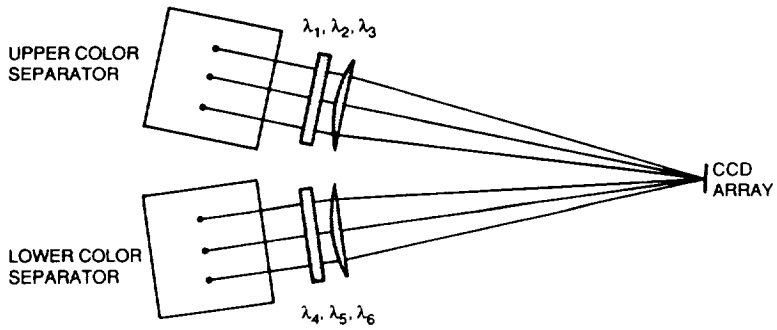

Figure 3. Side view of pyrometer optical configuration.

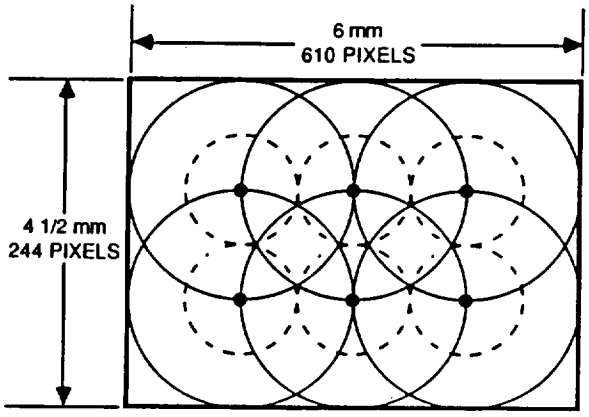

Figure 4. Arrangement of six images on CCD array. Solid circles enclose the area used to project onto the detector the entire field-of-view seen by each image. Dashed circles indicate the maximum size of a moving object that can be observed without suffering image overlap.

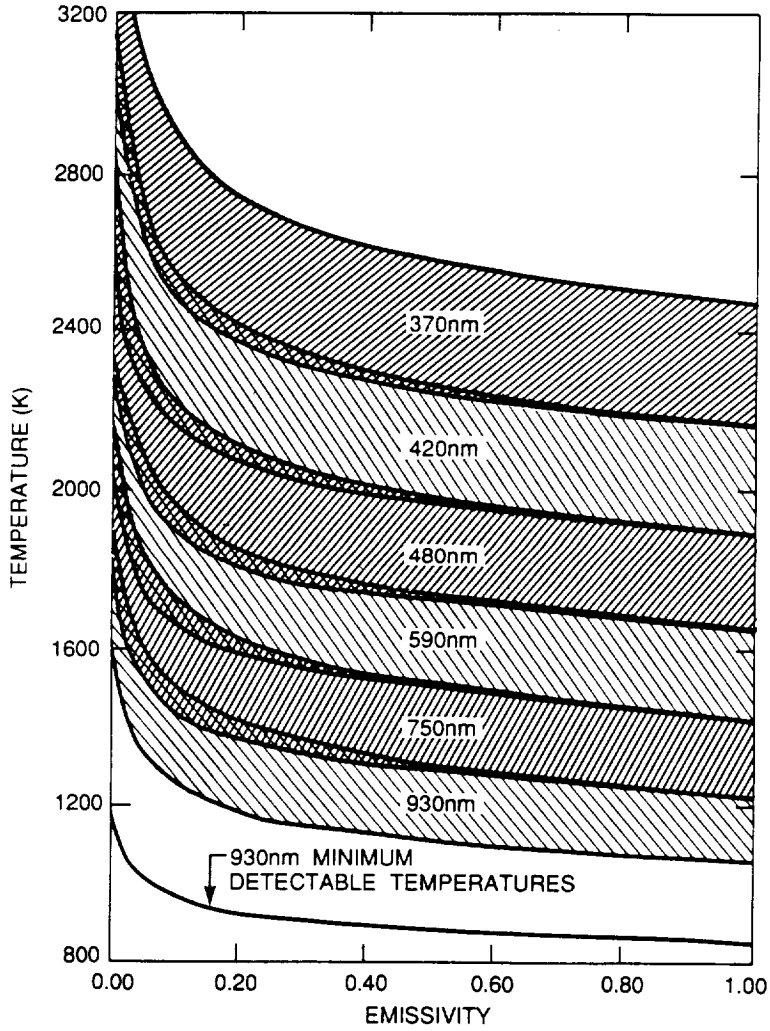

Figure 5. Temperature ranges observable at each wavelength as a function of sample emissivity.

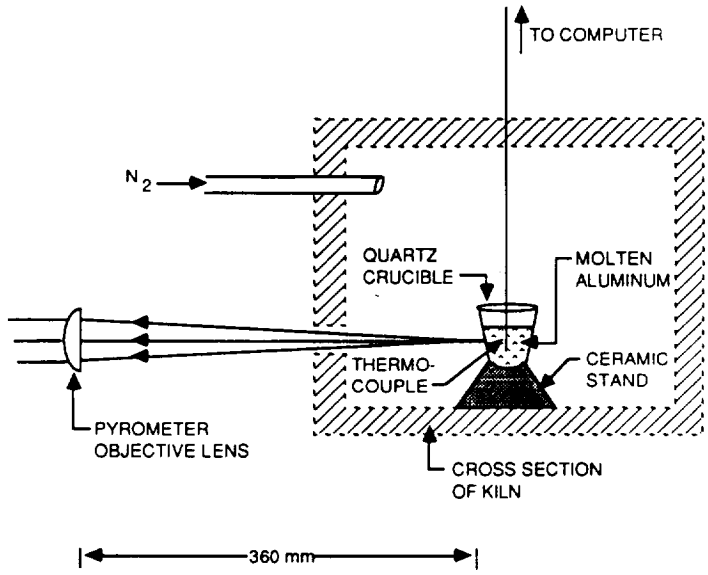

Figure 6. Illustration of pyrometer demonstration experiment.

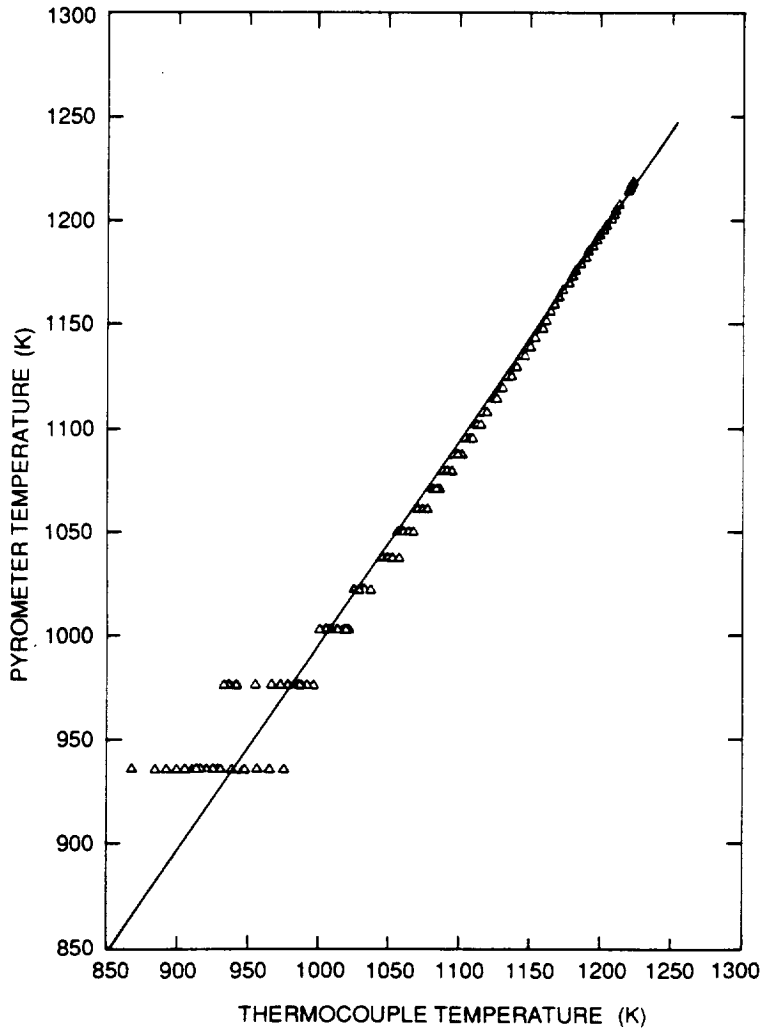

Figure 7. Comparisons of temperatures measured by a multicolor pyrometer vs those measured by thermocouple for molten aluminum heated in a kiln.